

The Comdined Effect of the Self Excited and External Forced Vibrations on the Pressure Disturbution of Short Journal Bearing.

Abdulkareem Abdulrazzaq

Huda Mseer Abdulkadum

Mechanical Engineering Department , University of Kerbala

Alhumdany@yahoo.com

hudasmile234@gmail.com

Abstract

The performance of the journal bearing at the dynamic loading condition under the effect of self-excitation and forced harmonic excitation has been investigated. For this purpose, the conventional form of the Reynolds equation is analyzed numerically using the central finite difference technique with a proper initial and boundary condition. The numerical equations have been written in (FORTRAN-95) language to obtain the results. According to the numerical results obtained, the maximum oil pressure is obtained under the combined effect of forced harmonic vibration and self-excitation is increased by 36.66 percent from those obtained under the self- excitation only.

Key words: Journal bearing, Reynolds equation, Forced harmonic vibration, Self- excitation

الخلاصة

تم دراسة أداء المحمل الزيتي في حالة التحميل الديناميكي تحت تأثير الإثارة الذاتية والإثارة التوافقية القسرية. ولذا، تم تحليل الشكل التقليدي لمعادلة رينولدز عددياً باستخدام تقنية الاختلاف المركزي المحدود ضمن حدود أولية محددة. وقد كتبت المعادلات العددية بلغة (فورتران-95) للحصول على النتائج. وفقاً للنتائج العددية التي تم الحصول عليها، وجد أن أقصى ضغط لزيت تحت التأثير المشترك للاهتزاز التوافقي القسري و الإثارة الذاتية إزدادت بنسبة 36.66 % من تلك التي تم الحصول عليها تحت الإثارة الذاتية فقط.

الكلمات المفتاحية: محمل زيتي، معادلة رينولدز، الاهتزاز التوافقي القسري، الإثارة الذاتية.

List of Abbreviations

| Symbol | Description | Units |
|-------------|--|---------|
| c | Bearing Radial Clearance | m |
| e | Eccentricity of Journal | m |
| E | The Modules Elasticity of the Material of the Shaft | N/m^2 |
| F | Amplitude of the Vibration Force | N |
| h | Oil Film Thickness | m |
| h_{max} | Maximum Oil Film Thickness | m |
| h_{min} | Minimum Oil Film Thickness | m |
| h_v | Oil Film Thickness Under External Vibration | m |
| \bar{h} | Dimensionless Oil Film Thickness (h/c) | |
| \bar{h}_v | Dimensionless Oil Film Thickness under External Vibration, $\bar{h}_v = \frac{h_v}{c}$ | --- |
| I | The Second Moment of Area = $\frac{\pi d^4}{64}$ | m^4 |
| i, j | The Indexes Increase a Long x, z Axes | --- |
| K | Stiffness of the Journal (Shaft) | N/m |
| L | Bearing Length | m |
| M | Mass of the Journal | kg |
| N | Journal Rotational Speed | rpm |
| P | Oil Film Pressure | MPa |
| \bar{P} | Dimensionless Oil Pressure = $\frac{p}{6\mu\omega} \left(\frac{c}{R}\right)^2$ | --- |

| | | |
|---------|--------------------------------------|-------|
| R | Journal Radius | m |
| R_1 | Bearing Radius | m |
| t | Time | sec |
| T | Non-dimensional time, $T = \omega t$ | --- |
| u | Linear Journal Speed | m/sec |
| x, y, z | Coordinate System | m |

Greek Symbols

| Symbol | Description | Units |
|---------------------|---|-------------------|
| ε | Eccentricity Ratio, $\varepsilon = \frac{e}{c}$ | --- |
| $\dot{\varepsilon}$ | Non-Dimensional Eccentricity Ratio Variation, $\dot{\varepsilon} = \dot{e}/c$ | --- |
| ξ | Damping Ratio | --- |
| μ | Lubrication Viscosity | Pa. s |
| ρ | Mass Density of Oil | Kg/m ³ |
| θ | Angular Co-ordinate Measured from the Line of Centers (The Circumferential Direction) | rad |
| φ | Bearing Attitude Angle | rad |
| $\dot{\varphi}$ | Time Rate of Attitude Angle | rad/sec |
| ψ | Phase Angle of Oscillation | rad |
| ω | Angular velocity, $\omega = \frac{2\pi N}{60}$ | rad/sec |
| ω_e | Excitation Frequency | rad/sec |
| ω_n | Journal Natural Frequency | rad/sec |

Superscript

| | |
|---|-------------------------------|
| — | Dimensionless quantity |
|---|-------------------------------|

1. Introduction

Hydrodynamic bearings are utilized to support rotating shafts of heavy machines. The sliding and rolling bearing elements are the two common sorts of bearings which are generally utilized as a part of rotor-bearing system applications. The sliding bearing (fluid film bearings) are utilized to support load in many engineering applications, such as internal combustion engines, airplane cylinder motors, and large steam turbines in power plants (**Uğur, 2005**).

Journal bearings are designed in such a way to reduce friction and to minimize wear and rupture risks, so that even in the worst conditions, journal and bearing are not expected to come in contact (**Paulo et.al., 2006**).

Journal bearings have a self-excited instability, which is generally called the self-excited oil whirl. The reason for the instability is due to the unbalance-induced vibration.

The vibration caused by mass unbalance, which is known as the self-excited vibration, is a significant factor restricting the performance and fatigue life of a rotating system (**Bouزيدane and Thomas, 2008**).

The main aim of this work is to determine the pressure distribution of short journal bearing due to the combined effect of self-excited and external harmonic excitation. Hence this paper includes the effect of the amplitude of external force, the frequency ratio and damping factor on the pressure distribution.

2. The Geometry and Coordinate of Journal Bearing System

For self-excited $h(\theta, t) = c(1 + \varepsilon \cos\theta)$

$$c = R_1 - R$$

where c is a radial clearance

h_{min} - minimum film thickness at $F = c - e$

h_{max} - maximum film thickness at $G = c + e$

ε - eccentricity ratio = e/c

When shaft and bearing are concentric $e = 0$

$$\varepsilon = 0$$

When the shaft and bearing are touch $e = c$

$$\varepsilon = 1$$

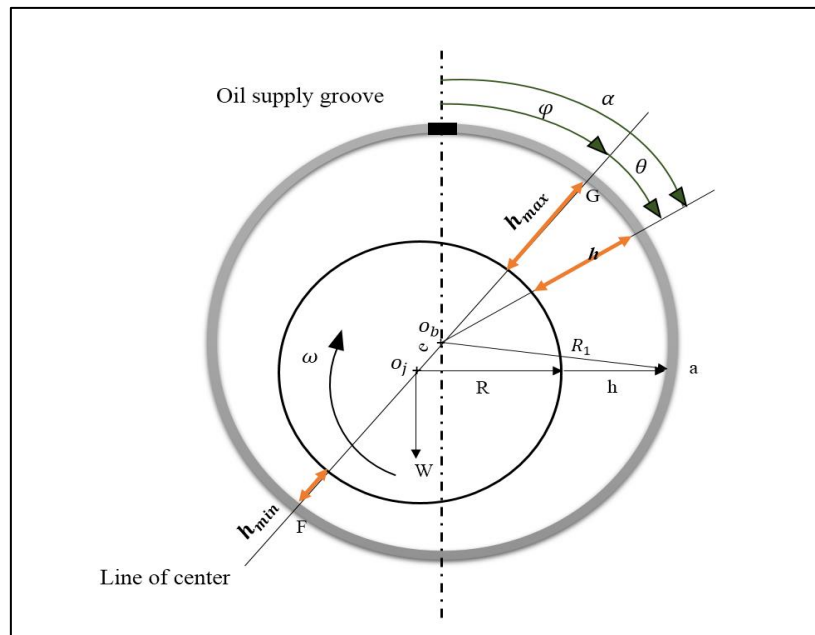


Figure (1) Geometry of Journal Bearing

And the global coordinates system used is to be Cartesian (x, y, z) with the original point fixed to bearing bush center, as it is shown in figure (2)

The x - coordinate is in the circumferential direction, y - coordinate across the oil film thickness, and the (z) coordinate in the axial direction, across the length of bearing perpendicular to the plane of (x, y)

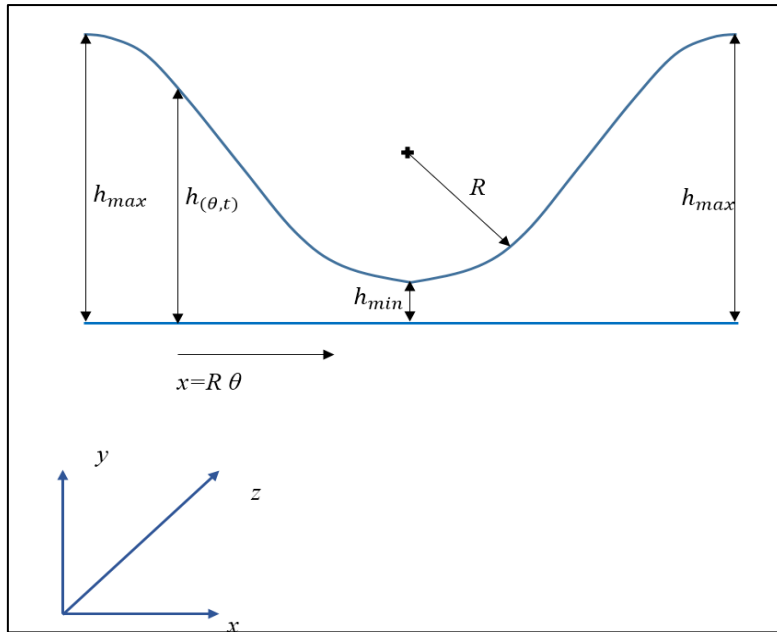


Figure (2) Oil Film Thickness and Coordinate of the System of Journal Bearing

3. Reynold's Equation

The Reynolds equation for the laminar flow of an isoviscous incompressible fluid is , (Uğur , 2005) :

$$\frac{\partial}{\partial x} \left(h^3 \frac{\partial p}{\partial x} \right) + \frac{\partial}{\partial z} \left(h^3 \frac{\partial p}{\partial z} \right) = 6\mu u \frac{\partial h}{\partial x} + 12\mu \frac{\partial h}{\partial t} \quad (1)$$

Using the short journal bearing theory based on the Ocivirk approximation (Paulo *et.al.*, 2006) . The Reynold equation will be:

$$\frac{\partial}{\partial z} \left(h^3 \frac{\partial p}{\partial z} \right) = 6\mu u \frac{\partial h}{\partial x} + 12\mu \frac{\partial h}{\partial t} \quad (2)$$

4. Solution of Reynold's Equation

The dynamic effect in tribology is meant to consider the effect of $(\partial h / \partial t)$ in Reynolds equation (Dowson , 1962). The dynamic effect is considered to be generated from two sources, namely

1. Self-excitation
2. Forced harmonic excitation

4.1 Analytical solution

When the journal bearing is subjected to external vibration such as a harmonic excitation the response will take the form of the particular integral.

The particular integral represents the response of the system to forced vibration, as expressed by (Singiresu , 2000), as,

$$h_2(t) = H_2 \sin(\omega t - \psi) \quad (3)$$

Where

H_2 and ψ are the amplitude of oscillation and the phase angle of the displacement with respect to the exciting force, respectively

$$H_2 = \frac{f}{K \sqrt{\left[1 - \left(\frac{\omega_e}{\omega_n}\right)^2\right]^2 + \left[2\xi \frac{\omega_e}{\omega_n}\right]^2}} \quad (4)$$

$$\psi = \tan^{-1} \frac{2\xi \frac{\omega_e}{\omega_n}}{1 - \left(\frac{\omega_e}{\omega_n}\right)^2} \quad (5)$$

where

$\frac{\omega_e}{\omega_n}$ – frequency ratio

To find the value of the stiffness (K); consider the journal bearing as a simply support beam and use the double integration method (Singiresu, 2000),

$$K = \frac{48EI}{L^3} \quad (6)$$

$$\omega_n = \sqrt{\frac{48EI}{ML^3}} \quad (7)$$

Assuming that, under external vibration the oil film thickness will be

$$h_v = h_1 + h_2 \quad (8)$$

Where

$$h_1(\theta, t) = h(\theta, t) = c(1 + \varepsilon(t)\cos\theta) \quad (9)$$

$$h_2(t) = H_2 \sin(\omega_e t - \psi) \quad (10)$$

The new equation of the oil film thickness under a harmonic excitation will be,

$$h_v(\theta, t) = c(1 + \varepsilon \cos\theta) + H_2 \sin(\omega t - \psi) \quad (11)$$

A gain for the right hand side of equation (2),

$$\frac{dh_v}{dx} = \frac{-c\varepsilon \sin\theta}{R} \quad (12)$$

$$\frac{\partial h_v}{\partial t} = c(\varepsilon \sin\theta \dot{\varphi} + \dot{\varepsilon} \cos\theta) + \omega H_2 \cos(\omega t - \psi) \quad (13)$$

Substituting equations (12) and (13) in to equation (2), and using the boundary conditions at the journal bearing edges (Gwidon and Andrew, 2001):

$$p = p_{atm} = 0 \quad \text{at } \theta = 0.2\pi \text{ and } z = \pm \frac{l}{2} \quad (14)$$

leads to the equation of oil film pressure distribution of journal bearing subjected to external vibration,

$$p = \frac{6\mu}{h^3} [c\varepsilon \cos\theta + c\varepsilon \sin\theta(\dot{\varphi} - \bar{\omega}) + \omega H_2 \cos(\omega t - \psi)] \left(z^2 - \frac{L^2}{4}\right) \quad (15)$$

4.2 Numerical Solution

The non-dimensional form of Reynold's equation (2) with constant viscosity is described as:

$$\bar{h}^3 \left(\frac{R}{L}\right)^2 \frac{\partial}{\partial \bar{z}} \left(\frac{\partial \bar{P}}{\partial \bar{z}}\right) = \frac{\partial \bar{h}}{\partial \theta} + 2 \frac{\partial \bar{h}}{\partial T} \quad (16)$$

Where:

$$\bar{P} = \frac{p}{6\mu\omega} \left(\frac{c}{R}\right)^2 \quad \bar{z} = \frac{z}{l} \quad \theta = \frac{x}{R} \quad T = \frac{tu}{R} \quad (17)$$

$$\bar{h} = \frac{h_v(\theta, t)}{c} = (1 + \varepsilon \cos\theta) + \frac{H_2}{c} \sin(\omega_e t - \psi) \quad (18)$$

The dimensionless governing differential equation described above is solved using the finite difference quotients to get the pressure distribution in the oil film.

4.2.1 Mesh generation

The dimensionless oil film pressure distribution can be also obtained by solving equation (16), which can be greatly simplified by a well – constructed grid. For short bearing approximation and for 2-D finite difference analysis, a grid size is chosen to be (n) in circumferential direction, θ and (m) in axial direction, z, as it is shown in figure (3). The central technique in the finite difference method is adopted.

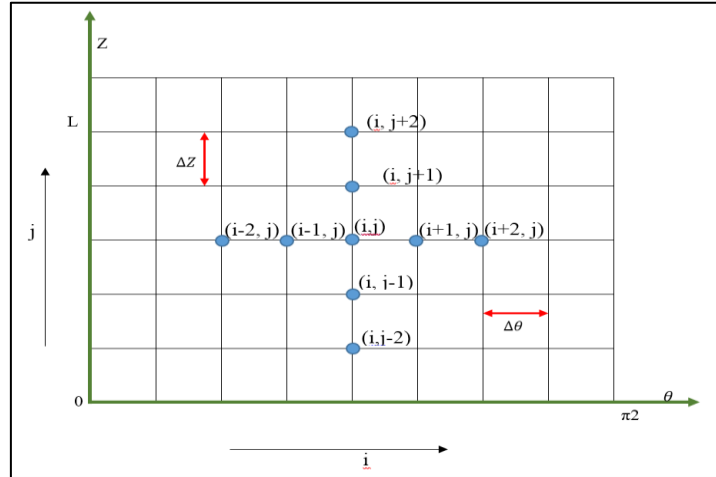


Figure (3) Discretization of Oil Film Domain

$$1 \leq i \leq n, 1 \leq j \leq m$$

The mesh size in circumferential direction (Δx) and along the bearing length (Δz) is defined as:

$$\Delta x = \frac{2\pi R}{n-1} \quad (19)$$

$$\Delta z = \frac{L}{m-1} \quad (20)$$

which can be expressed in a dimensionless group as:

$$\Delta \theta = \frac{\Delta x}{R} \quad (21)$$

$$\Delta \bar{z} = \frac{\Delta z}{L} \quad (22)$$

4.2.2 Solution of the Reynold's Equation

To get the pressure distribution (\bar{P}) through the oil film, the grid points are taken in both the coordinates of θ and \bar{z} .

For any point in the oil film mesh (i, j), the Reynold equation can be written as:

$$\bar{h}_{i,j}^3 \left(\frac{R}{L} \right)^2 \left(\frac{\bar{P}_{i,j+1} - 2\bar{P}_{i,j} + \bar{P}_{i,j-1}}{\Delta \bar{z}^2} \right) = \frac{\bar{h}_{i+1,j} - \bar{h}_{i-1,j}}{2\Delta \bar{x}} + 2 \left(\frac{\bar{h}_{i,j}^{n+1} - \bar{h}_{i,j}^n}{\Delta T} \right) \quad (23)$$

$$\begin{aligned} & (\bar{P}_{i,j+1} - 2\bar{P}_{i,j} + \bar{P}_{i,j-1}) \\ &= \left[\left(\frac{\bar{h}_{i+1,j} - \bar{h}_{i-1,j}}{2\Delta \bar{x}} \right) + 2 \left(\frac{\bar{h}_{i,j}^{n+1} - \bar{h}_{i,j}^n}{\Delta T} \right) \right] \left[\frac{(L/R)^2 \Delta \bar{z}^2}{\bar{h}_{i,j}^3} \right] \end{aligned} \quad (24)$$

Rearranging equation (24) for $\bar{P}_{i,j}$:

$$\bar{P}_{i,j} = \left[\frac{\bar{P}_{i,j+1} + \bar{P}_{i,j-1}}{2} \right] - \left[\left(\frac{\bar{h}_{i+1,j} - \bar{h}_{i-1,j}}{2\Delta \bar{x}} \right) + 2 \left(\frac{\bar{h}_{i,j}^{n+1} - \bar{h}_{i,j}^n}{\Delta T} \right) \right] \left[\frac{(L/R)^2 \Delta \bar{z}^2}{\bar{h}_{i,j}^3} \right] \quad (25)$$

The equation above gives the dimensionless oil film pressure in the circumference and axial directions.

5. Results and Discussion

The results of solving the Reynold equation numerically are discussed using the data listed in table (1).

Table (1) The Journal Bearing Characteristic of the Case Study

| Parameter | Symbol | Unit | Value |
|-----------------------|---------------|-------|----------|
| Journal dimeter | D | m | 0.05 |
| Bearing length | L | m | 0.025 |
| Radial clearance | c | m | 0.000025 |
| Rotational speed | N | rpm | 4000 |
| Lubrication viscosity | μ | Pa .s | 0.00416 |
| eccentricity ratio | ε | — | 0.58 |

Figure (4) shows the maximum oil film pressure dynamically loaded with and without the effect of forced vibration as a function of time. It is observed that the maximum oil film pressure increases in the case of the combined effect. The percentage of this increment is 36.662 %. The fluctuating trend is attributed to the sinusoidal nature of load in the harmonic excitation.

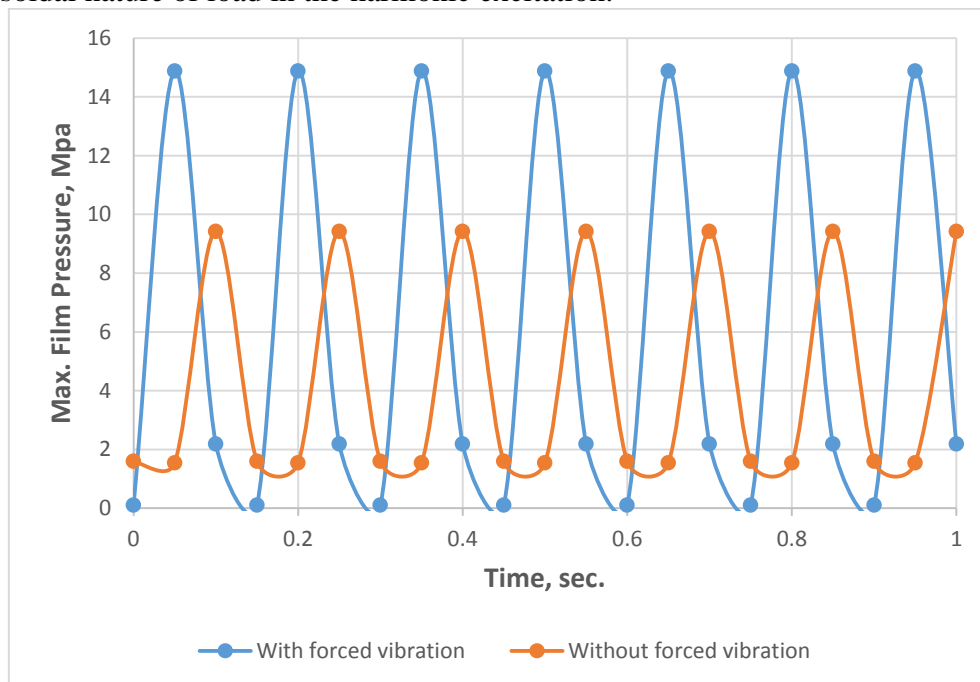


Figure (4) Maximum Pressure Distribution of the Journal Bearing with and without Forced Vibration Effect During 1 sec

Figure (5) shows the distribution of oil film pressure during a certain time along the circumferential direction. It is found that the increase in the amplitude of the vibration force causes the pressure to be increased.

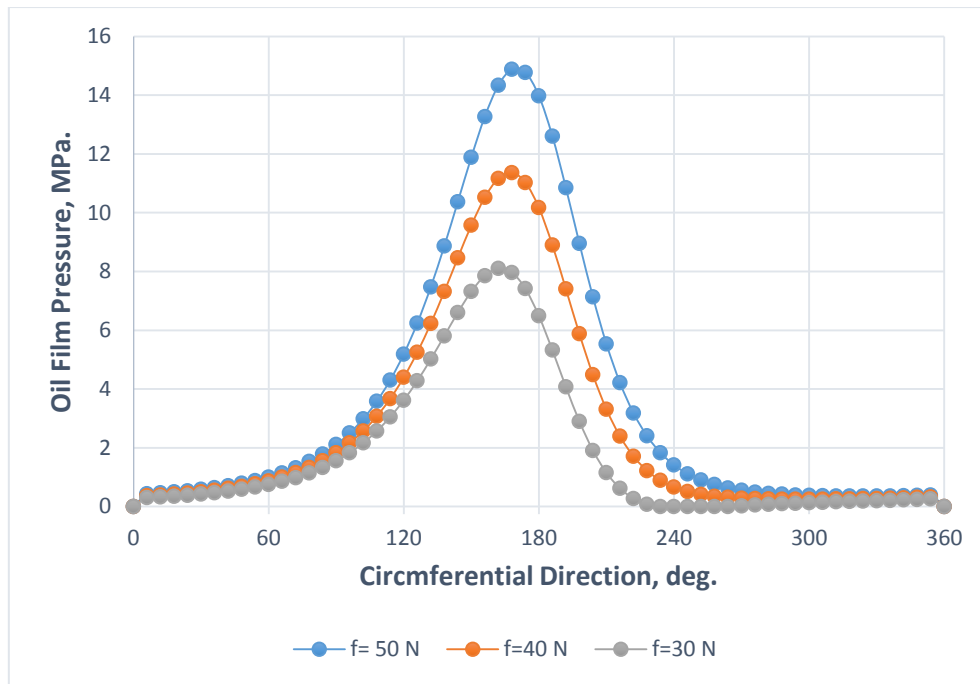


Figure (5) Oil Film Pressure for Different Values of Amplitude of Forced Vibration

Figure (6), shows the variation of the maximum oil film pressure with the damping ratio for different values of ω_e/ω_n ratio.

It is observed that for $\frac{\omega_e}{\omega_n} < 1$, the maximum oil film pressure decreases significantly with the increase of the damping ratio. While for $\frac{\omega_e}{\omega_n} > 1$, the effect of the damping ratio on the maximum oil film pressure is little.

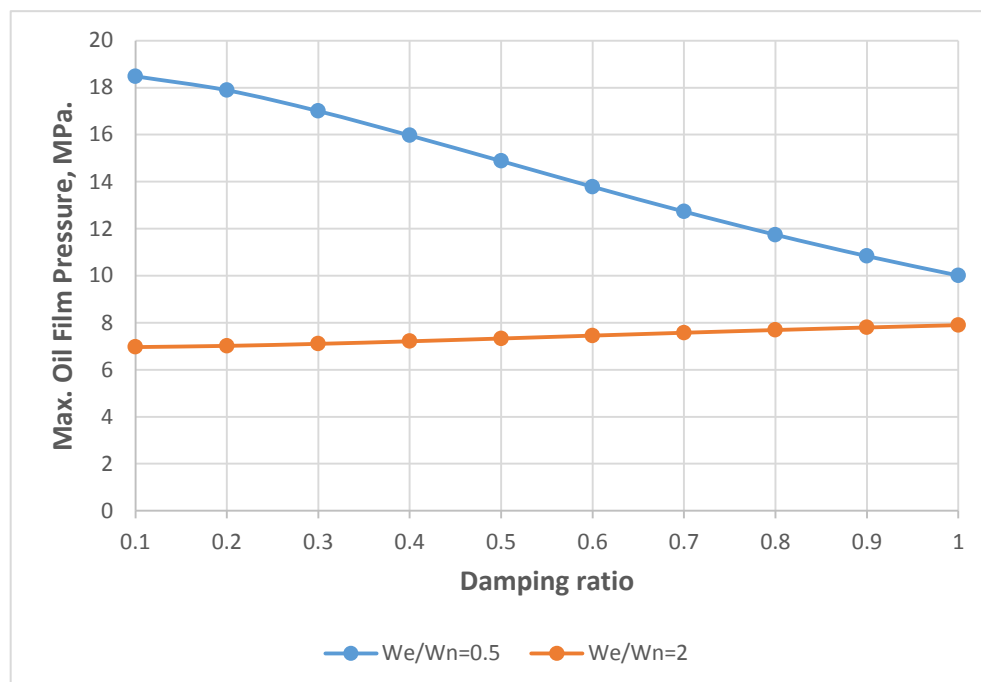


Figure (6) Maximum Pressure Distribution Versus Damping Ratio for Different Values of (ω_e/ω_n) .

Figure (7) show the variation of the maximum oil film pressure with time for different values of damping ratio. It can be concluded that as the damping ratio increases, the maximum pressure decreases. This is due to the fact that the damping dissipates the energy of vibration and then it decreases the amplitude of vibration response.

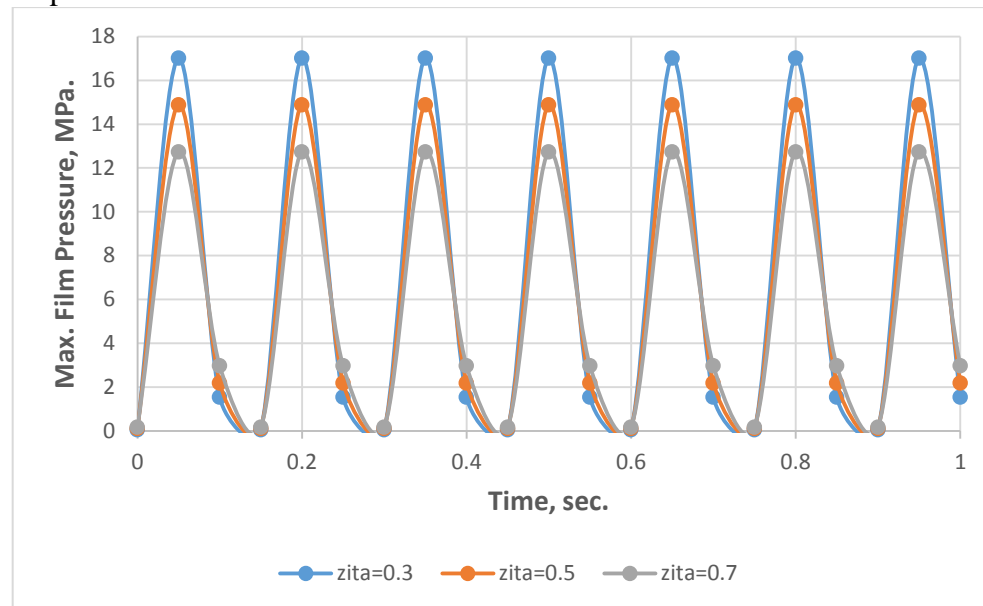


Figure (7) Maximum Oil Film Pressure for Different Values of Damping Ratio During 1 sec.

Figure (8) shows the variation of maximum pressure with time for different values of frequency ratio. It can be noticed that for the higher frequency ratio the maximum pressure decreases. While for the low frequency ratio, the maximum pressure increases. This can be attributed to the fact that the increase in the frequency ratio leads to the increase in the minimum oil film thickness causing the oil film pressure to be decreased.

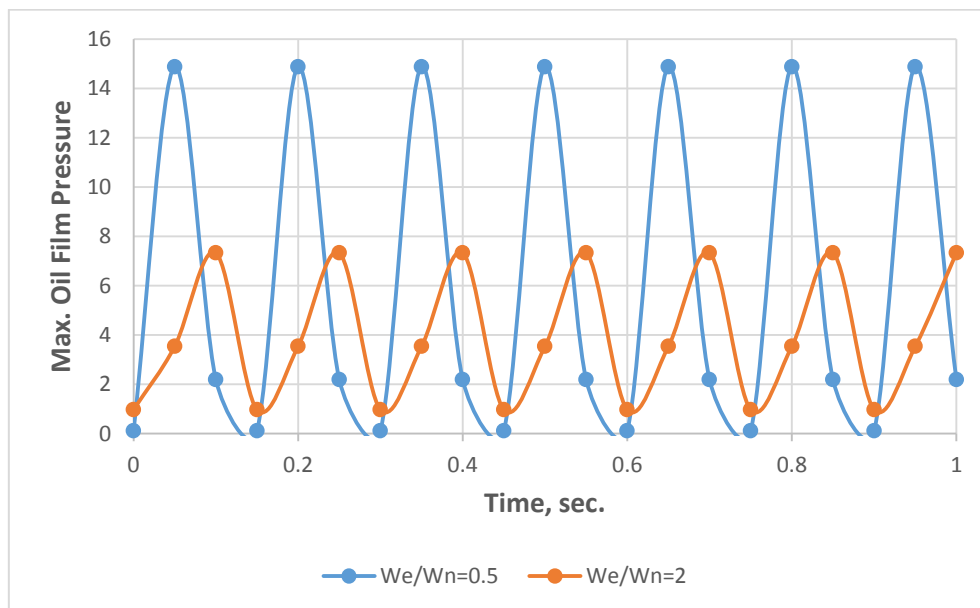


Figure (8) Maximum Oil Film Pressure Distribution for Different Values (ω_e/ω_n) During 1 sec

Figure (9) shows the maximum oil film pressure and minimum film thickness as a function of time. A little change in oil film thickness causes a significant variation in the film pressure. It can also be noticed that a sinusoidal fluctuation of the oil film pressure results from the sinusoidal nature of oil film thickness

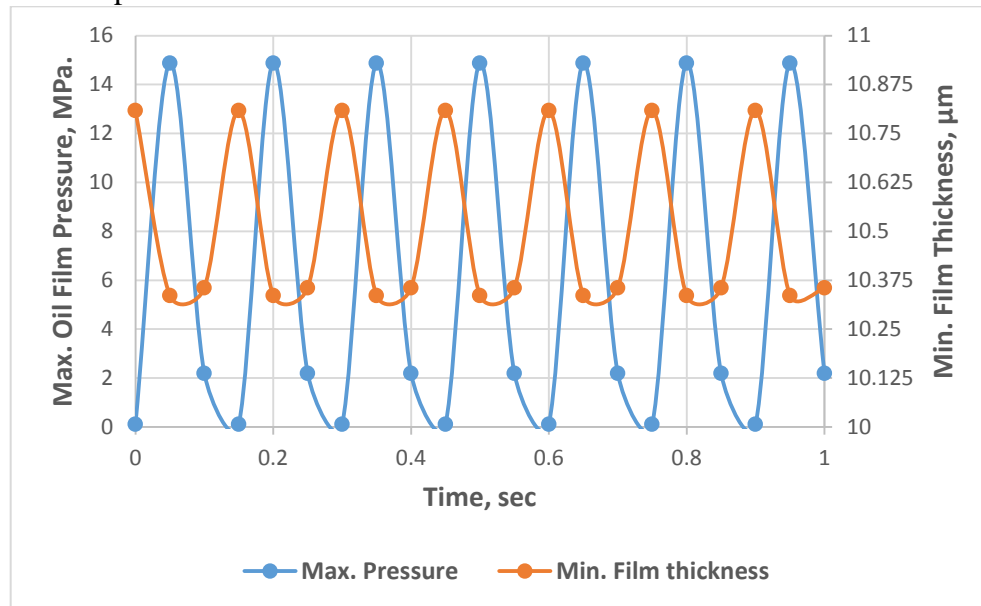


Figure (9) Maximum Oil Film Pressure and Minimum Film Thickness Variation During 1 sec.

Figure (10) shows the minimum film thickness versus damping ratio for different value of ω_e/ω_n . It is observed that for the higher frequency ratio, the increase in the damping ratio has no considerable effect on the minimum film thickness. While for the low frequency ratio, the minimum oil film thickness increases considerably with the increase of the damping factor leading to a decreases in the oil film pressure.

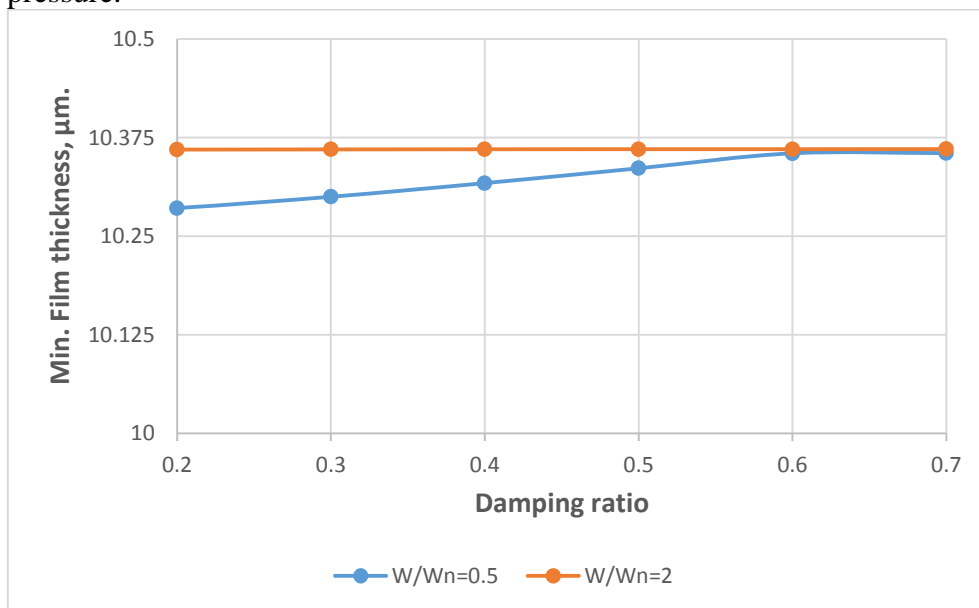


Figure (10) Minimum Film Thickness Versus Damping Ratio for Different Values of (ω_e/ω_n)

Figure (11) shows the oil film pressure distribution under the combined effect of self-excited vibration and forced harmonic excitation in three dimensions. It can be

observed that the maximum value of the oil film pressure (14.8778 MPa) occurs at ($\theta = 168$ deg.) at the central plane of bearing.

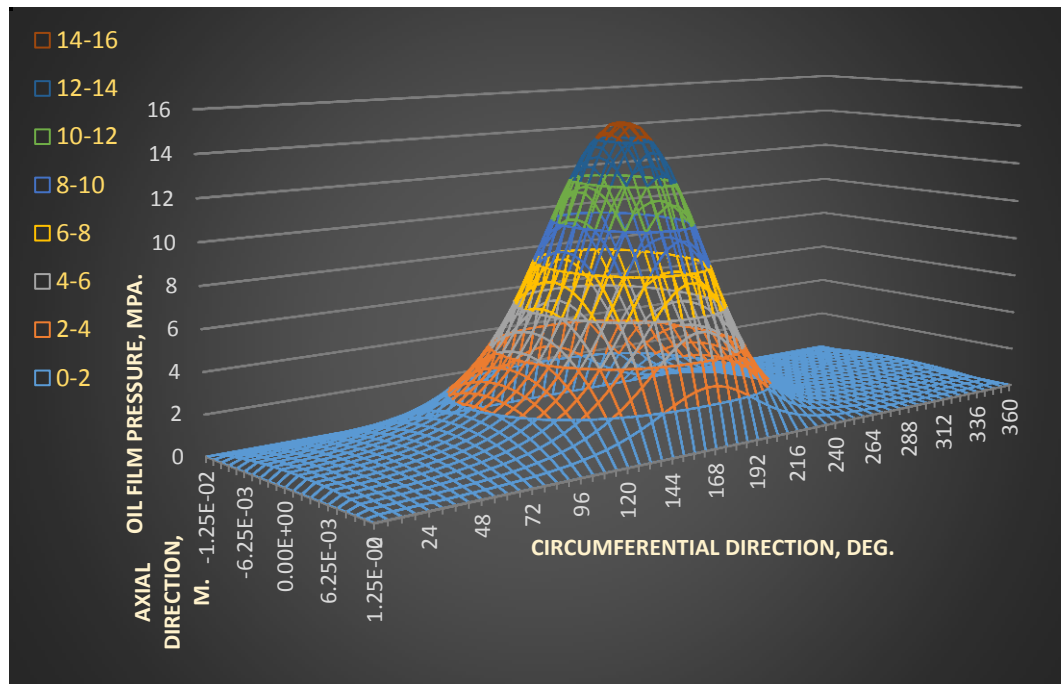


Figure (11) Oil Film Pressure Distribution Along the Circumferential Direction of Journal Bearing in 3- Dimension.

6. Conclusions

The following conclusions can be withdrawn:

1. The maximum oil film pressure increases under the effect of the combined case as compared to the effect of self-excited only by (36.66 %).
2. The oil film pressure increases as the amplitude of vibration force increases
3. The oil film pressure decreases for large the value of damping ratio up to 0.7
4. The oil film pressure decreases for ($\frac{\omega_e}{\omega_n} > 1$), while it increases for ($\frac{\omega_e}{\omega_n} < 1$).

References

- Bouزيدane A., Thomas M.**, 2008, "An electrorheological hydrostatic journal bearing for controlling rotor vibration", Computers and Structures, Vol 86, pp. 463-472.
- Dowson D.**, 1962, "A generalized Reynolds equation for fluid film lubrication", Int.J.Mech.Sci.Vol.4 pp.159-170.
- Gwidon W. Stachowiak and Andrew W. Batchelor**, 2001, "Engineering Tribology", 2'nd, Utter worth Einemann, Australia.
- Paulo Flores, JC Pimenta Claro and Jorge Ambrósio**, 2006, "Journal Bearing Subjected to Dynamic Loads, The Analytical Mobility Method", Mechanica Experimental, Vol 13, pp. 115-127.
- Singiresu S. Rao**, 2000, "Mechanical Vibrations", 2'nd, Addison- Wesley Publishing Company.
- Uğur YÜCEL**, 2005, "Calculation of Dynamic Coefficient for Fluid Film Journal Bearings", Journal of Engineering science, Vol 11, No 3, pp. 335-343.